LJMU Research Online

Khidasheli, N, Gvazava, S, Zakharov, G, Chikhradze, M, Batako, ADL, Ahuir-Torres, JI, Pazhani, A and Xavior, MA

 Effect of Heat Treatments on the Microstructure, Corrosion Resistance and Wear Behaviour of Bainitic/Martensitic Ductile Iron Under Dry Sliding Friction

https://researchonline.ljmu.ac.uk/id/eprint/26448/

Article

For more information please contact researchonline@ljmu.ac.uk

Effect of Heat Treatments on the Microstructure, Corrosion Resistance and Wear Behaviour of Bainitic/Martensitic Ductile Iron Under Dry Sliding Friction

Nugzar Khidasheli [1], Salome Gvazava [1], Garegin Zakharov [2], Mikheil Chikhradze [2], Andre Danonu Lignamnateh Batako [3,*], Juan Ignacio Ahuir-Torres [3], Ashwath Pazhani [4] and Micheal Anthony Xavior [5]

1   Faculty of Chemical Technology and Metallurgy, Georgian Technical University, Kostava Street 77, Tbilisi 0160, Georgia; khidly@gtu.ge (N.K.); s.gvazava@bk.ru (S.G.)
2   Ferdinand Tavadze Metallurgy and Materials Science Institute, Mindeli Street 8b, Tbilisi 0186, Georgia; algar12@mail.ru (G.Z.); m.chikhradze@gtu.ge (M.C.)
3   The General Engineering Research Institute, School of Engineering, Faculty of Health, Innovation, Technology and Science, Liverpool John Moores University, Byrom Street, Liverpool L3 3AF, UK; j.i.ahuirtorres@ljmu.ac.uk
4   Faculty of Engineering, Environment and Computing, Coventry University, Coventry CV1 5FB, UK; ae0255@coventry.ac.uk
5   School of Mechanical Engineering, Vellore Institute of Technology, Vellore 632014, India; manthonyxavior@vit.ac.in
*   Correspondence: a.d.batako@ljmu.ac.uk

Abstract: The development of high-strength cast irons with multiphase metal matrix structures is one of the new areas of modern materials science and mechanical engineering. This is so because of the high dissipative properties of such materials, which, in turn, ensure an improvement in their functional characteristics. It is known that one of the effective methods for obtaining alloys with a heterogeneous structure is a multi-stage heat treatment. Therefore, this study aimed to enhance the corrosion and friction properties of high-strength cast irons by combining different processing methods to create a bainite-martensitic matrix. High-strength cast irons with high ductility micro-alloyed with boron were chosen as the object for research. The experiments studied the effect of various types of multi-stage heat treatment on the structural features, tribological properties, hardness and corrosion resistance. The cast irons were quenched in water or liquid nitrogen after a controlled duration of isothermal exposure at different temperatures. It was established that cooling of isothermally hardened samples in liquid nitrogen makes it possible to effectively engineer the morphology and amount of the formed martensitic phase. It was observed that the high-strength cast irons with 10–15% lower bainite, residual austenite and martensite have the best frictional characteristics. This innovative method allowed the quenching of cast iron directly into liquid nitrogen without violent cracking.

Keywords: ductile cast iron; alloying; corrosion; tribology; microstructure design; nitrogen cooling

1. Introduction

The automotive brake systems operate in extreme conditions, thus, during their design and development, one must take these conditions into account so that these systems have high mechanical strength, corrosion, temperature and wear resistance, as well as an optimal coefficient of friction. Therefore, it is important to select a new class of innovative

structural materials, such as high-strength cast irons with various types of bainite matrix. The functional properties of these materials are formed through multiple methods of heat treatment, which determines the purposeful control of the morphology and ratio of structural components, taking into account the conditions of their operation [1–5]. This is due to the fact that depending on the design features, braking force and duration, temperature conditions, the wear resistance of the brake system materials and the braking performance can vary significantly. The reliability of braking and the durability of friction pairs can only be ensured with a balanced ratio of metal matrix components [6–8]. The combination of various methods of heat treatment and microalloying of liquid iron makes it possible to obtain alloys with a multiphase structure, which are characterized by higher dissipative properties and contribute to the uniform distribution of external dynamic loads [9–13].

This explains the advantages of high-strength bainite cast irons. The heterogeneous structure can be adapted to various frictional and corrosion loading conditions [14].

This is achieved using variations of multi-stage isothermal hardening, resulting in a regulation of the ratio of different bainite types and residual austenite [15–17].

The paper notes that, in order to improve the tribological properties of bainitic cast irons, it is better to combine high-strength martensite and crack-resistant lower bainite in the structure of their metal matrix [18–21].

An increase in the specific volume of martensite in relation to specific austenite is accompanied by an enhancement in the corrosion resistance of the high-strength cast iron [22]. The efficiency and mechanism of influence of the martensitic phase on the functional properties of bainite-martensitic cast irons depends on the sequence of formation of their structural components [23].

Preformed martensite strengthens the metal matrix, but it can accelerate subsequent bainite transformation and promote the formation of ultrafine bainite in the residual austenite [24–28]. If the initial decay of the initial austenite proceeds according to the bainite mechanism, then at the subsequent stage of structure formation, the volumes of residual austenite can only be strengthened due to dispersed martensite crystals. The kinetics of the metal matrix hardening processes depend on the carbon enrichment degree of the initial austenite and the technological parameters of the process. The martensitic transformation temperature is diminished with the increase in the carbon concentration for the austenite phase and the Ni additives. It limits the effectiveness of martensitic quenching of high-strength cast irons [29–32].

Cast iron is known to belong to the group of high-carbon brittle materials characterized by low crack resistance since their grain boundaries are saturated with undesirable chemical compounds such as sulphides, nitrides, carbides, etc. This makes it difficult to treat cast iron with deep cryogenic because doing so induces significant internal stresses and increases the generation and spread of microcracks.

The high-strength cast irons micro-alloyed with boron deserve attention. The microalloying of the melt (liquid metal) with boron introduces peculiarities into the formation of the structure and complex of high-strength cast iron properties [33]. In particular, [33,34], the microalloying of high-strength cast iron with boron improves the tribological properties and provides stability in the friction coefficient due to the formation of finely dispersed boron compounds in the structure. Boron (0.005–0.01%) micro-alloyed iron castings have higher thermal cyclic strength and fatigue life, as well as low sparking during braking.

It has been established [35] that the influence of boron micro-additives increased the corrosion resistance in Fe-C alloys under conditions of cyclic oxidation. This is due to the fact that the oxidation of iron borides is slower [36–40]. The use of boron micro-additives

instead of Ni, Cu and Mo is more economically feasible, which increases their commercial competitiveness.

The combination of direct and isothermal hardening methods can allow the design of the mechanism and kinetics of phase transformations for the high-strength cast irons. This can permit the formation of new heterogeneous structural compositions with high friction, wear and corrosion resistance. However, the processes and parameters of structure formation are scarcely studied in the literature.

For the purposeful design of multiphase bainite-martensitic structures, the presented work here studied the influence of various thermal variants on the decay patterns of the initial austenite. The functional properties (friction, wear and corrosion resistance) of high-strength irons with boron micro-alloy were also the aim of the study.

2. Experimental Setup

2.1. Materials

Standard cast iron of the following composition C- 4.20%; 1.8% Si; 0.25% Mn; 0.03% S and 0.04% P were used as raw material along with scrap steel and were smelted in an induction furnace MGP-102 with a crucible capacity of 50 kg. To activate the graphite nodules to form spheroidal shapes, magnesium was injected into the liquid cast iron melt at 1320–1330 °C. After spheroidization was completed, the molten metal was superheated to 1550 °C, where boron micro-additives were added. After a thorough mixing, the liquid metal was poured into sand moulds. Table 1 gives the chemical composition of the obtained products.

Table 1. Chemical composition.

	Chemical Composition of High-Strength Cast Iron, %						
	C	Si	Mn	S	P	B	Mg
Basic	3.42	2.12	0.31	0.005	0.005	-	0.040
Boron alloyed	3.45	2.20	0.25	0.003	0.06	0.03	0.045

2.2. Heat Treatment Cycles

In order to obtain various phase components in the metal matrix of cast irons, the experimental samples were heat-treated according to the Time-Temperature Isothermal Transformation Diagram-TTT Diagram, [41]. However, in this work, the heat treatment was conducted using specifically designed thermal cycles illustrated in Figure 1, which schematically shows diagrams of the beginning of isothermal decay of the original austenite. The duration of isothermal hardening of the samples and the temperatures (280 °C and 400 °C) were also determined and shown in this figure. The TTT diagrams, though standard, were constructed using magnetic-thermal analysis for this newly developed micro-alloyed ductile iron to assist in understanding the process.

For the austenitization, the cast irons were heated up to 900 °C then held for 60 min (Figure 1a) and for 120 min in (Figure 1b). This was followed with an isothermal quenching at a temperature 400 °C (Figure 1a) and 280 °C (Figure 1b) in a liquid bath of Pb-Bi-Sn alloy. After a controlled holding for set intervals of time (5–15 min), the samples were quenched in water or liquid nitrogen. The isothermal quenching modes were selected specifically to obtain structural compositions of martensite with various types of bainite crystals. For example, isothermal quenching at 400 °C ensures the disintegration of the initial austenite by the diffusion mechanism with the formation of upper bainite. Due to the increase in the duration of the phase transformation, the amount of bainite phase in the metal matrix of cast irons increases, while the stability of residual austenite increases, which affects its

further decomposition by the martensitic mechanism during subsequent cooling in water or in liquid nitrogen (LN).
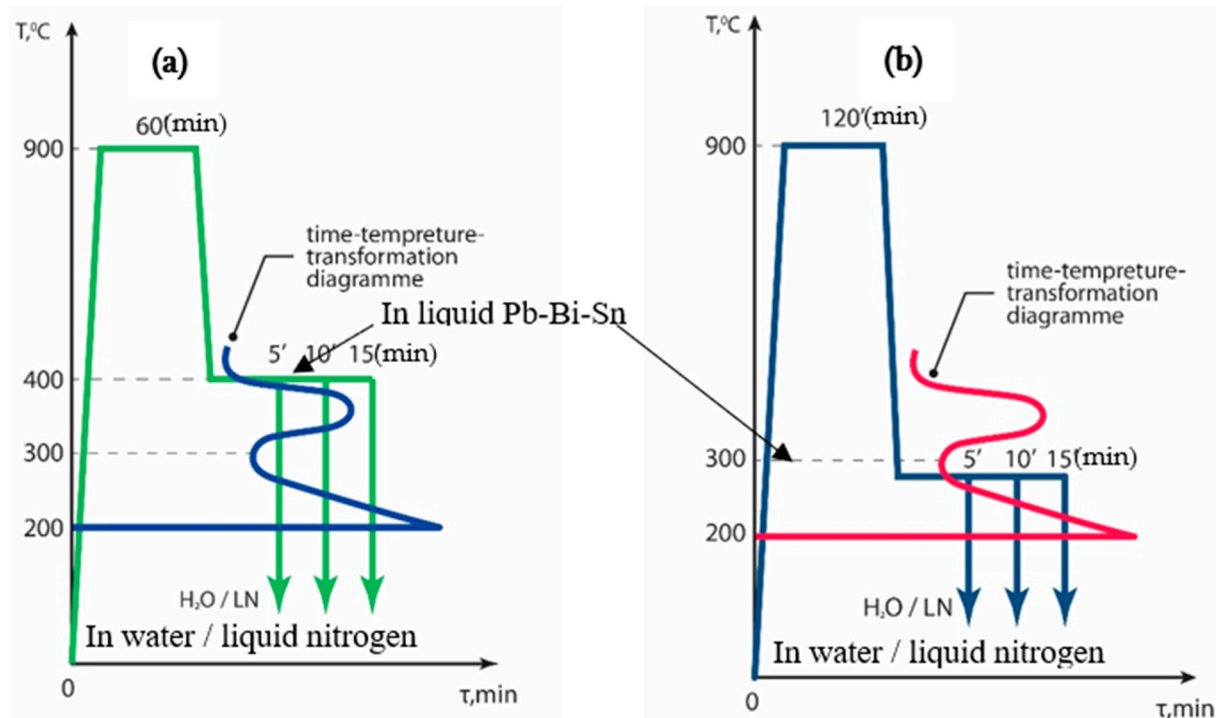

Figure 1. Schematic diagram of heat treatment processes.

The isothermal quenching at 280 °C contributed to the disintegration of the initial austenite by the shear mechanism with the formation of lower bainite crystals. The cooling of the samples after controlled exposure for 5–15 min in water or liquid nitrogen led to the formation of a mixture of lower bainite and martensite.

The selected treatment processes provided the martensitic hardening of cast irons with bainite matrix at various stages of the process. It should be pointed out that cooling the cast iron samples from high temperatures directly in liquid nitrogen is a challenging process, which is usually associated with violent cracking of the specimen, see Figure 2a. However, Figure 2c shows the process used in this work, where a sample was taken from the furnace at 400 °C and quenched directly into liquid nitrogen; Figure 2b shows the polished sample after cooling, and Figure 2d illustrates a magnification of the sample surface and no cracks are observed. This supports the soundness of this new method of high-temperature direct quenching in liquid nitrogen. Figure 2c is given here to illustrate the process, though it is blurred due to the vapour of liquid nitrogen.

During this process, one must pay attention to the formation of an undesired gaseous layer that covers the sample. To prevent the formation of this layer, the sample was rapidly moved into the quenching liquid, and while being agitated, the sample was continuously spun until the end of the process. However, one could achieve sane results by spinning the sample until the boiling and bubbling of the nitrogen stops completely.

2.3. Microstructures Examination

The samples were etched in a 3% nital solution (3% nitric acid + 96% ethyl alcohol. Then, the microstructures of the heat-treated samples were studied using a Neophot 32 (Carl Zeiss, Jena, Germany) metallographic microscope. The phase analysis of the structure was carried out on a magnetometer and a diffractometer DRON-4 (ALROSA-Group). Subsequently, the hardness of the samples was measured on the Rockwell scale.
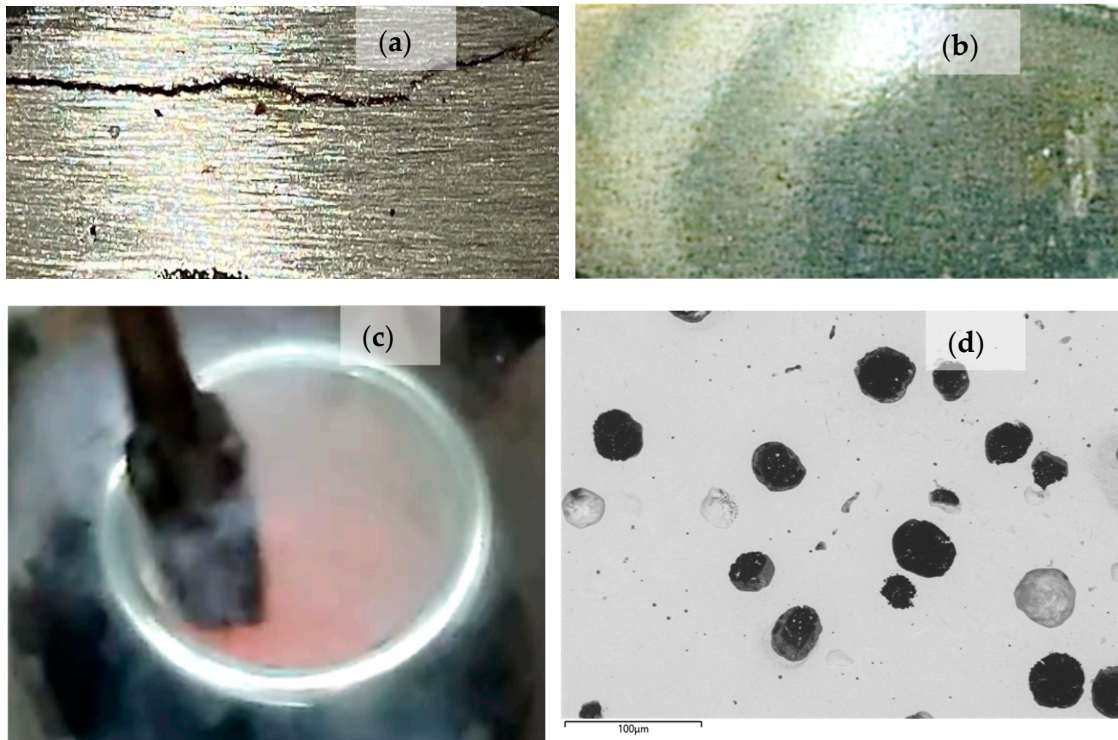
Figure 2. A sample directly from the oven at 400 °C being quenched into liquid nitrogen; (**a**) cracked conventional cast iron quenched in liquid nitrogen; (**b**,**d**) surface of modified and micro-alloyed cast iron quenched in liquid nitrogen; (**c**) process of quenching a sample in liquid nitrogen.

2.4. Corrosion Tests

Before the corrosion tests, all the test samples were weighed on a gravimetric scale with 0.04 mg accuracy. The samples were placed in refractory containers in a muffle furnace, as illustrated in Figure 3, and the temperature was raised homogeneously across the furnace up to 500 °C. During the experiment, the samples were periodically removed from the furnace every 168 h and weighed, which made it possible to record their weight. The intensity of corrosion processes was assessed by the increase in the weight of cast irons. The corrosion test took 1600 h to be completed.

2.5. Wear Tests

The dry slip wear tests were carried out using a conventional tribometer model SMC-2—"segment on disc", and the configuration is illustrated in Figure 4. The system was set to maintain a constant unidirectional sliding speed between the segment and the disc.

Here, a hardened carbon steel disc with 0.9% carbon and a hardness of 62 HRC was used as a counter-body. The normal loads applied were 20 N and 100 N, the sliding speed was 2.3 m/s and the total sliding distance was 6280 m without lubrication. After each continuous sliding run distance of 1256 m, the samples were removed from the system, cleaned and weighed to record the mass loss of the samples. The wear of the samples was measured by weight loss, and during each test the change in the coefficient of friction was also recorded, and the results are depicted in the respective section. The temperature was measured with a thermocouple inserted into the sample. A data acquisition (DAQ) was used to record all the signals on the connected computer.

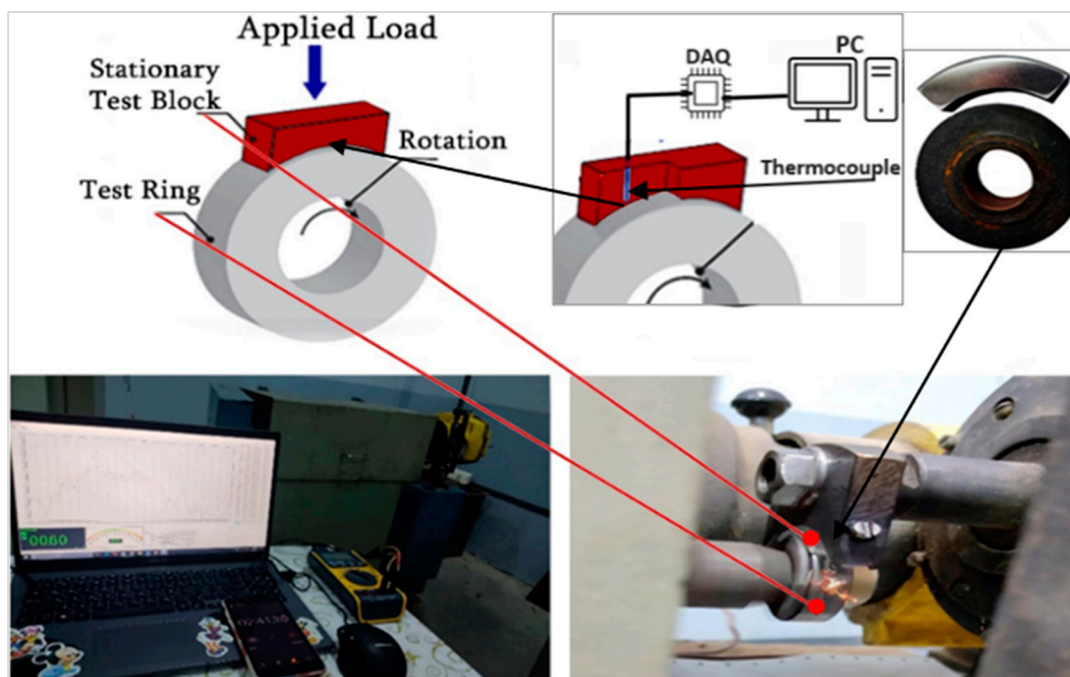**Figure 3.** Configuration for the high temperature corrosion test at 500 °C.

Figure 4. Friction and wear of experiment device.

3. Results and Discussion

One of the objectives of the study was to micro-alloy cast irons with 0.03% B to achieve various types of bainite-martensitic matrix. A residual austenite of 10 to 30% was observed in the structure as a result of heat treatment. The microstructural analyses of the samples indicated the effectiveness of the combined heat treatment methods that allowed for regulating the ratio of structural components of the metal matrix. In particular, with an

increase in the exposure of samples in the intermediate holding temperature range (280 °C or 400 °C), regardless of the mechanism of decay of the original austenite, the volume fraction of residual austenite decreased and became stable. This is due to a decrease in the amount of martensitic phase, which is formed as a result of cooling the cast iron in water or liquid nitrogen at later stages of the structure formation process. This new innovative micro-alloying with subsequent, direct quenching at relatively high temperatures contributed to a complete decomposition of the residual austenite and the hardening of the bainitic metal matrix, inducing dispersed inclusions of martensite.

3.1. Microstructural Study

The microstructural investigation was undertaken, and Figure 5 shows a typical SEM image of bainite-martensitic ductile iron obtained at 400 °C isothermal, followed by quenching in water, its key chemical components and the X-ray output. The SEM microstructure (Figure 5) shows that because of the isothermal tempering of ductile iron micro-alloyed with boron, disoriented crystals of upper bainite and block residual austenite are formed in the base metal.
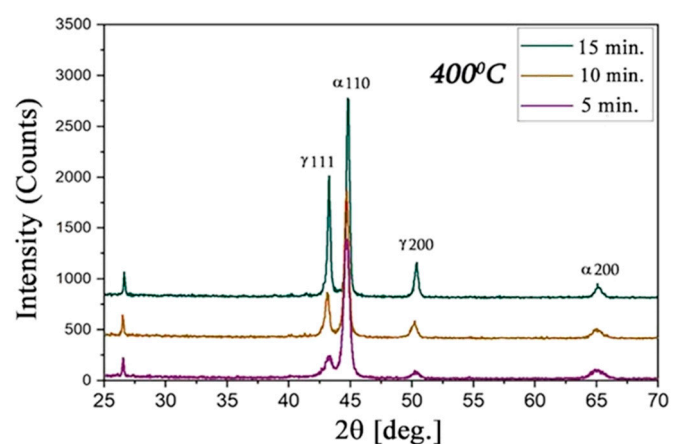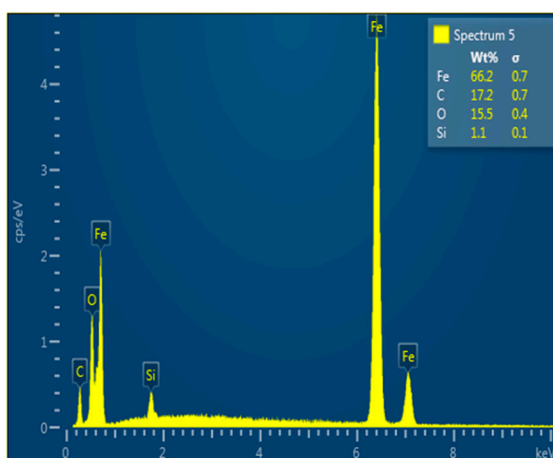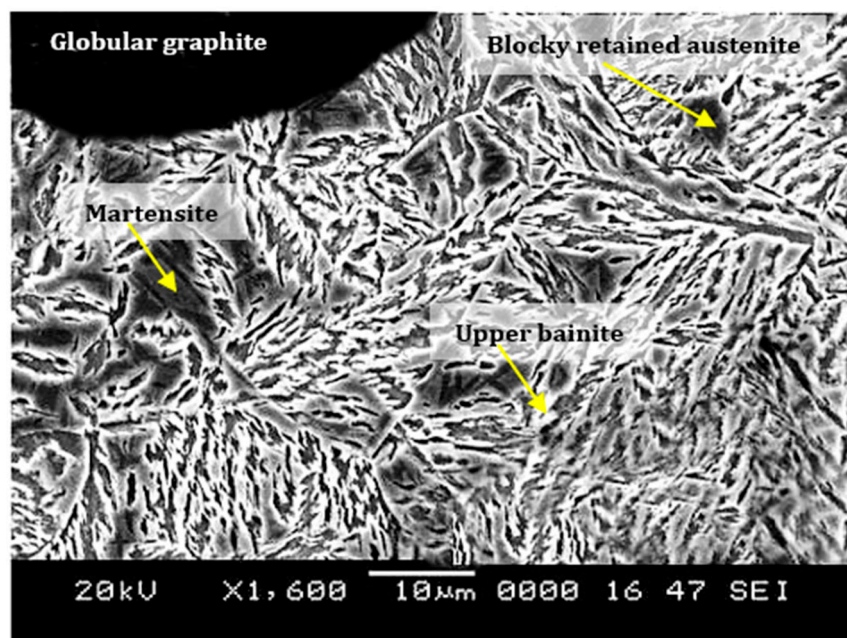

Figure 5. A typical SEM image of bainite-martensitic ductile iron.

Figure 6 illustrates the controlled formation of microstructures for various conditions using this novel technique of holding samples at 280 °C and 400 °C with subsequent quenching in water or liquid nitrogen. Here, one can observe the globular shape of the graphitic nodules, along with martensite, and lower and upper bainite. This is more evident in the strengthening of structures formed as a result of the disintegration of the initial austenite by the diffusion mechanism. One observes distinctive structures between the samples quenched in water and liquid nitrogen of the alloyed cast iron treated at 280 °C. The size and distribution of spherical graphite nodules and metal matrix components differ from each other, which is consistent with the difference in hardness of the samples. Similar behaviour is observed in samples treated at 400 °C.

3.2. Hardness Performance

The designed cast irons were also characterised by their hardness performance as a function of heat treatment. Figure 7 illustrates the hardness of samples as a function of isothermal holding time. One observes here that the samples quenched in liquid nitrogen have higher hardness than those hardened in water. Nitrogen-quenched samples show an average increase of 14% in hardness. However, with the increasing holding time, there is a linear decrease in hardness proportionally to the content of residual austenite, which causes a reduction in the hardness of the metal matrix.

3.3. Friction Coefficient

The engineered specimens with different structures were tested for wear resistance with unidirectional continuous dry sliding. Their performance depends on the bainite matrix type and the residual austenite amount. The samples with a multiphase bainite-martensitic matrix were characterised by more stable performance. This is seen with samples isothermally hardened at 400 °C, having an average friction coefficient of 0.4 (Figure 8a), whereas those treated at 280 °C show a coefficient of 0.28, as illustrated in Figure 8b.

Compared with bainite, cast irons alloyed with a multiphase bainite-martensitic matrix, a more stable friction coefficient, characterised the frictional load conditions, see Figures 9 and 10. This is explained by the hardening of residual austenite by dispersed inclusions of martensite, which causes the resistance of the cast iron matrix to deformation hardening and slows down the processes of its degradation and damage.

To record the weight losses over 6000 m of sliding distance, the samples were removed periodically at each 1256 m from the tribometer for weighing purposes and then placed back into the system. This process affected the samples with plain bainite structures; as they cooled down, their surface structures changed, leading to increased surface friction when placed back into the test rig. This is observed in Figures 9 and 10, as a step increase at the instant where the samples were placed back in the tribometer as shown in zone a) in Figure 10. As the sample heated up during the process, one observes a decrease in the friction coefficient for a couple of reasons.

Though the coefficient of friction fluctuated under repeated loading, yet, the high-strength cast irons with 10–20% of the bainite phase exhibited better performance, regardless of the mechanism of bainite formation, as shown in Figure 9a for 400 °C and Figure 9b for 280 °C with an average friction coefficient of 0.7 and 0.3, respectively.
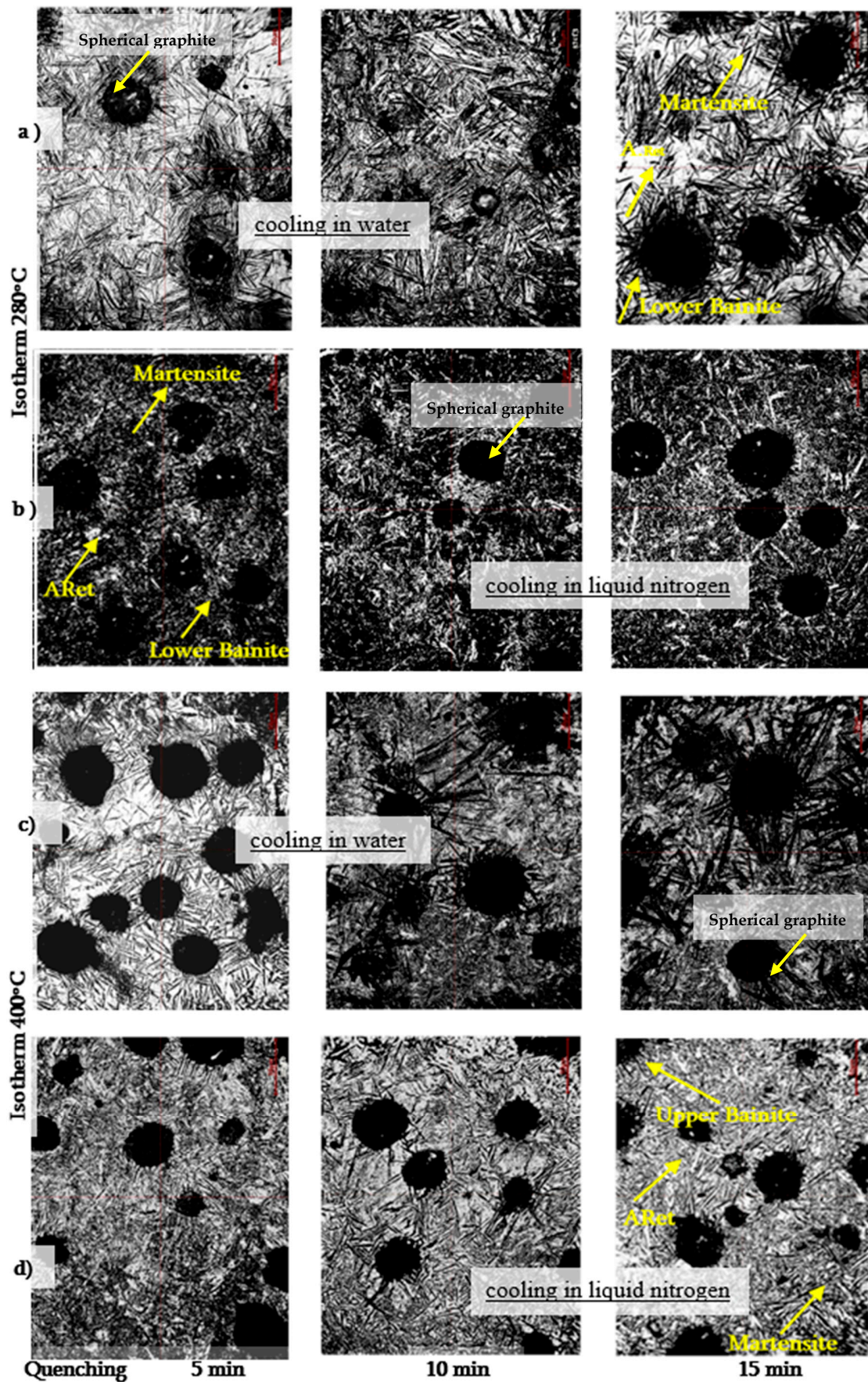
Figure 6. Samples microstructure at ×400 magnification after isothermal holding at temperatures of 280 °C (**a**,**b**) and 400 °C (**c**,**d**) and cooling in water (**a**,**c**) and liquid nitrogen (**b**,**d**).
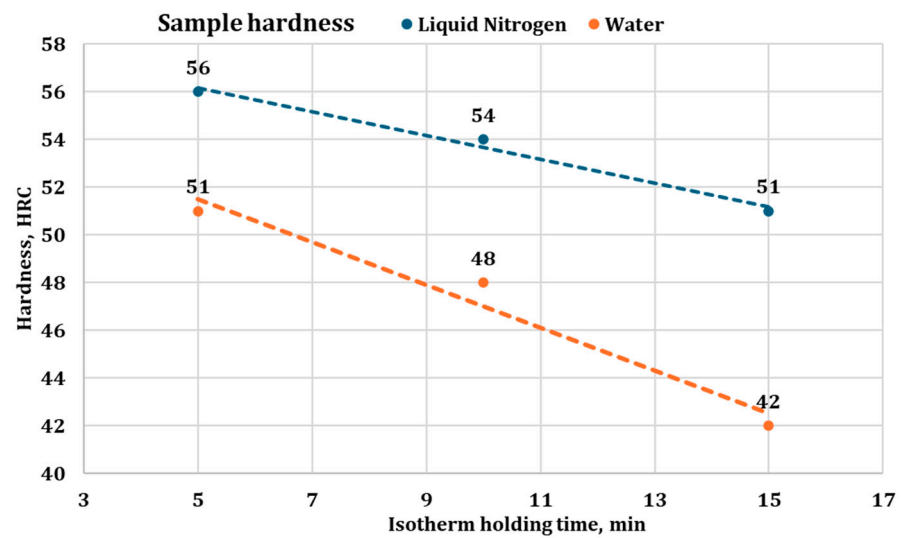
Figure 7. Samples hardness as a function of isothermal holding time at 280 °C.
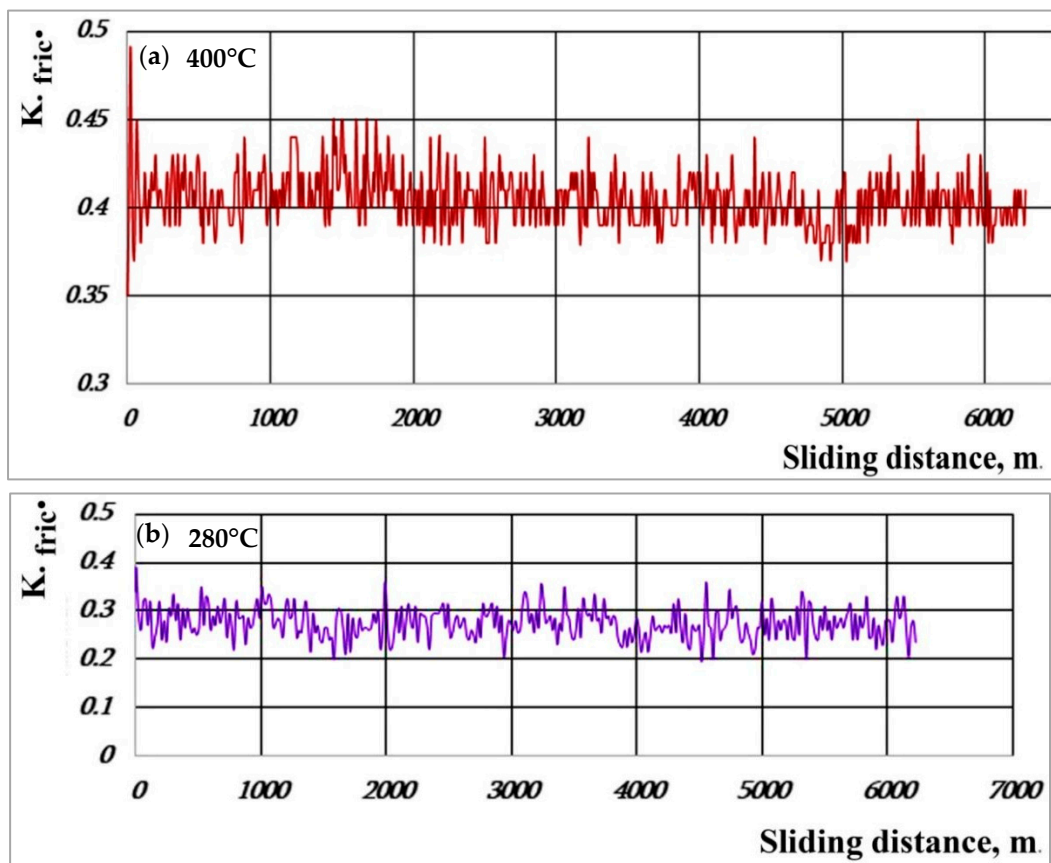
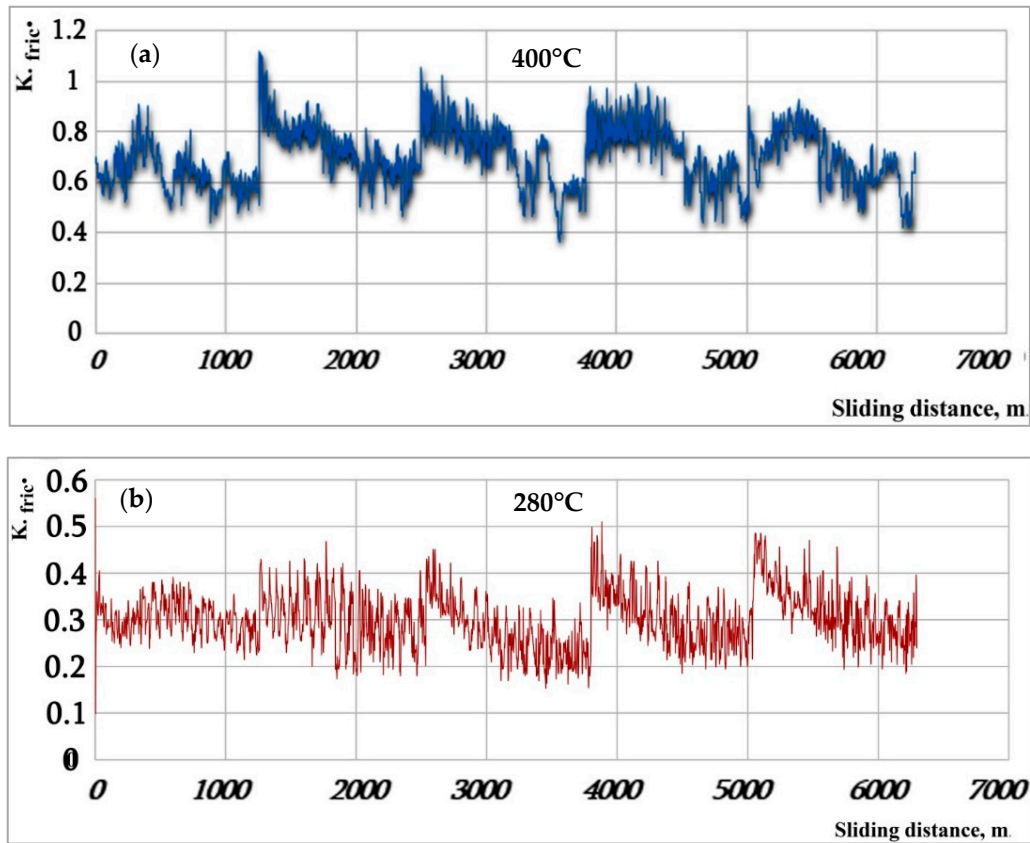**Figure 8.** Friction coefficient of bainite-martensitic cast irons isothermally hardened at 400 °C (**a**) and 280 °C (**b**).

Figure 9. Variation in friction coefficient of bainite ductile irons isothermally hardened at 400 °C (**a**) and 280 °C (**b**).

Zone-a): increased surface hardness due to cooling.

Zone-b): decreasing friction due to heat and solid lubrication

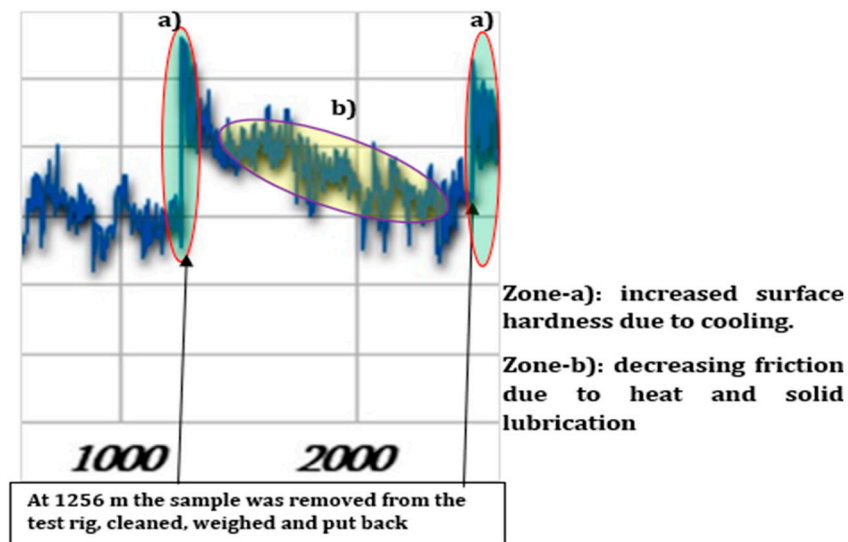At 1256 m the sample was removed from the test rig, cleaned, weighed and put back

Figure 10. Effect of cooling during the cleaning and weighing process.

The periodic frictional loading caused the samples to be reheated at each stage of the experiments to temperatures up to 300–520 °C depending on the axial load, the amount of residual austenite and the type of bainite matrix Figure 11.
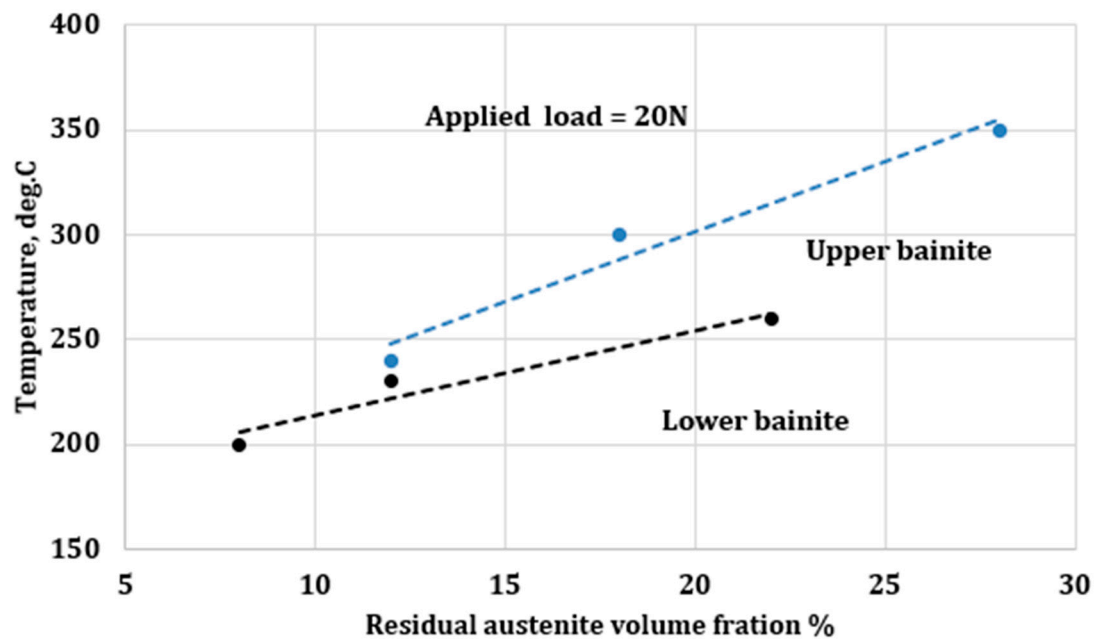
Figure 11. Friction temperature as a function of residual austenite and bainite type after 1000 m continuous dry sliding.

The increase in temperature in the friction contact zone contributes to the cyclic plastic deformations of the surface layers, with subsequent fatigue failure of the friction surface. The debris is gradually expelled out of the contact zone, and the graphitic nodules are exposed in the contact zone, as shown in Figure 12. The exposed graphic nodules are smeared over the contact zone and work as a lubricant, decreasing the friction coefficient. One could promulgate that the deformations occurring at the interface of the contacting surfaces at elevated temperatures led to an intermittent and combined smearing of residual austenite and graphitic elements in the contact zone. Figure 12 depicts the worn surface of tested samples, where one can see the brittle fracture of the surface layer exposing the granular graphitic nodules, which act as solid lubricant in the contact zone.
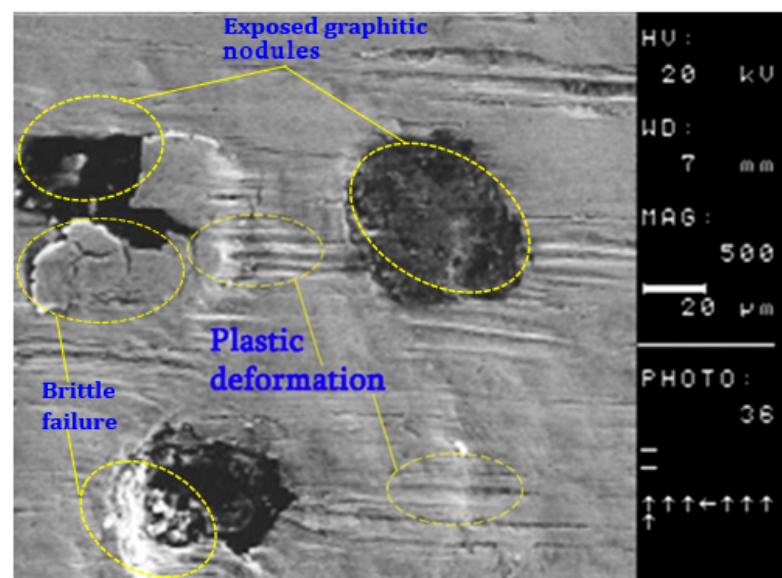

Figure 12. SEM-image of worn surfaces of tested samples.

3.4. Wear Performance

An increase in the ratio of the bainite and martensitic phases led to a decrease in wear resistance (Figure 13). Longer holding time for bainitic transformation induced an increase in the stability of residual austenite, but it decreased the amount of residual austenite. Consequently, longer holding time led to a decrease in the volume fraction of the martensitic phase in the metal matrix and the level of hardening. It is observed that the heterogeneous structures with a mixture of lower bainite and martensite had a higher frictional resistance. It can be stipulated that this is due to a positive combined effect of the physical and mechanical properties of the structural components.
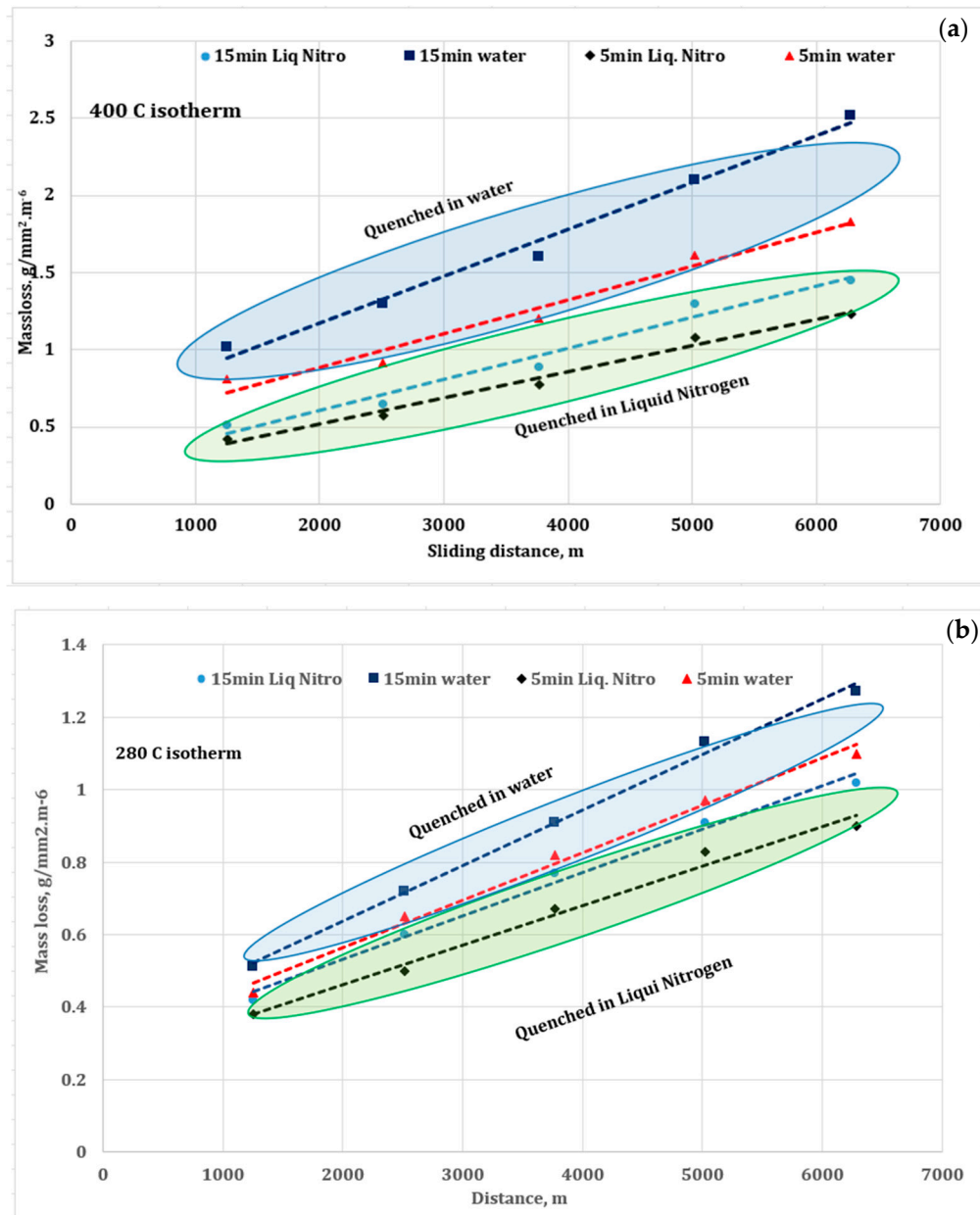

Figure 13. Wear resistance of bainite-martensitic ductile irons isothermally hardened at 400 °C (**a**) and 280 °C (**b**) for 5 min and 15 min.

3.5. Process Temperature

During the experiments, the temperature profile of the friction pair was measured using chromel/alumel thermocouples, as illustrated in Figure 4. This allowed for the quantifying of contact temperatures between 300 °C and 520 °C.

The results showed that the temperatures in the contact zone of friction pairs with identical structural characteristics mainly depend on the contact loads. Figure 14 depicts the contact temperatures as a function of loads over 1256 m, where the samples were removed from the test rig for weighing purposes. Here, one sees that the frictional temperature increased rapidly up to 400 m and then stabilised after that point until the end of the test.
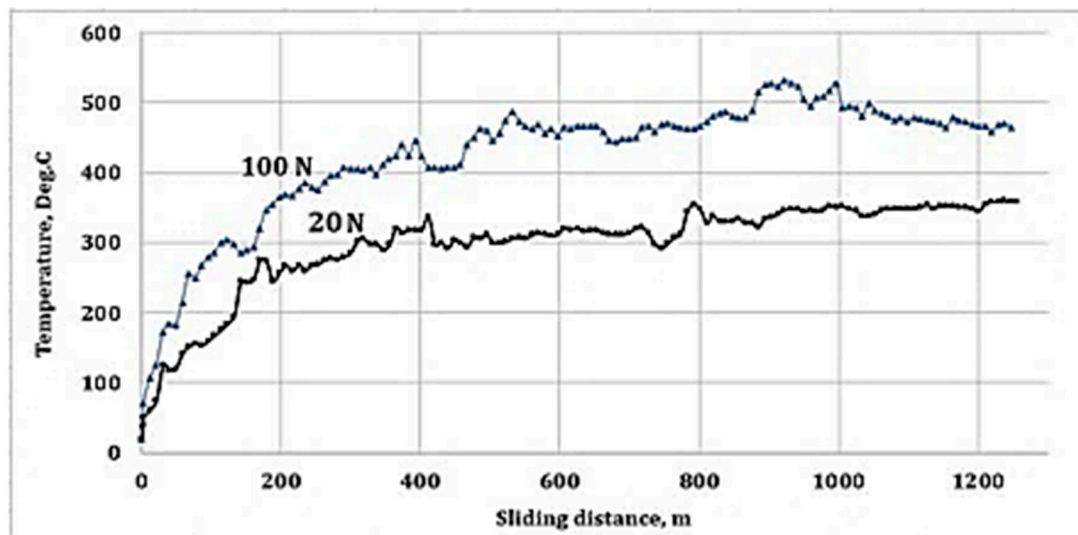

Figure 14. Contact temperature in the friction zone during dry sliding wear.

The associated high temperatures contributed to the intensification of oxidative processes and the formation of a thin layer of iron oxides, mainly hematite, at the surface of cast irons. The examination of oxide layers under a scanning electron microscopic (SEM) shows that the formed thin films have low density and mechanical stability, which limit their protective properties and do not effectively affect their corrosion and wear-resistant properties.

Figure 15 portrays the structure of the oxide layer, which is radically different from the bulk material illustrated in Figure 6 above. Since the oxide films were very thin, they were removed by the frictional process as wear products, exposing the original bulk material. The topographic analysis of friction surfaces showed no micro-cracks on the surface of the bainitic cast irons alloyed with boron caused by cyclic temperature fluctuations.

3.6. Corrosion Test

Here, the work focused on the corrosion process of boron micro-alloyed samples at a high temperature, 500 °C. An accelerated corrosion rate of all samples was observed during the first 250 h of the testing due to the rapid formation of the oxidised layer. From 300 h onwards, the formation of the oxidised layer stabilised, and Figure 16 depicts the corrosion performance.
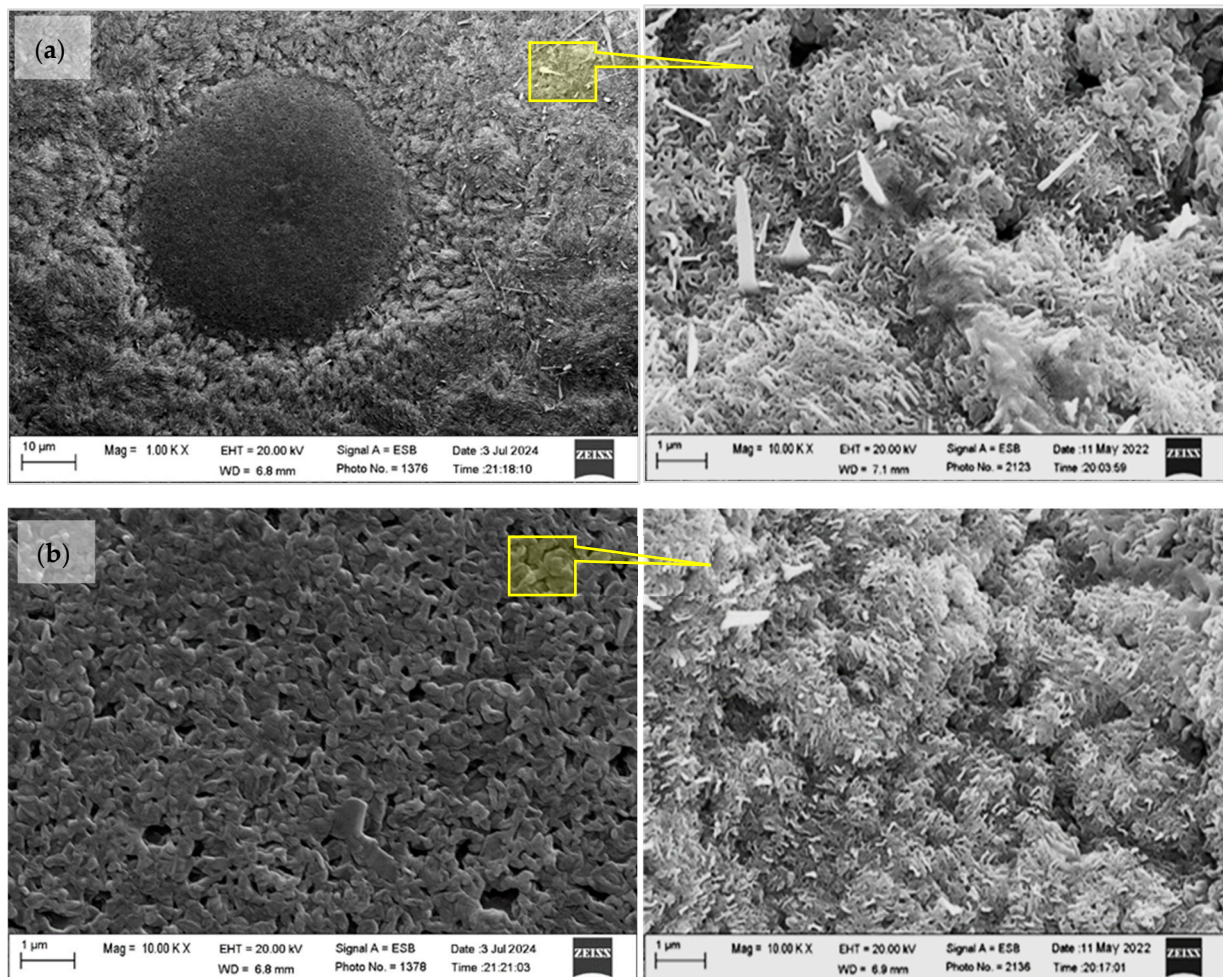
Figure 15. The oxide film formed on bainitic cast iron hardened at 280 °C, with 10% (**a**) and 40% (**b**) of residual austenite.
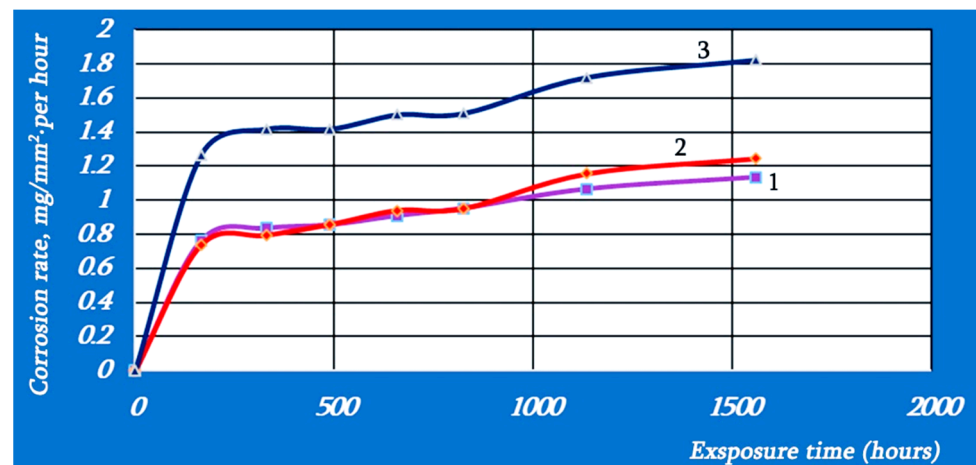

Figure 16. Corrosion performance under high temperature exposure (1)—5 min hold at 280 °C and cooled in liquid nitrogen; (2)—5 min hold at 280 °C and cooled in water; (3)—5 min hold at 400 °C and cooled in water.

The corrosion rate was calculated using the equation:

$$K = \frac{M_1 - M_0}{s \cdot \tau}, \ \frac{\text{mg}}{\text{mm}^2 \cdot \text{hour}};$$

K—is the corrosion rate, mg/mm^2·hours;

M_1—is the mass of the sample after the corrosion test, mg;

M_0—is the initial mass of the sample, mg;

S—is the area of the sample, mm^2;

τ—duration of the corrosion test.

The results in Figure 16 show that in the high-temperature corrosive environment, the samples with lower bainite quenched in liquid nitrogen had the lowest corrosion rate. They performed approximately 1.3–1.5 times better than the samples with an upper bainite matrix. This is due to the high dispersion of the metal matrix, the density of interfacial and intergranular boundaries and their lower diffusion permeability.

3.7. Remarks from Wear and Corrosion Test

One observes from the results of corrosion and wear tests that specimens held at 280 °C isotherm performed better in both tests compared to those at 400 °C. This is because at higher temperatures, i.e., 400 °C, there is more perlite in the matrix, which forms sets of galvanic pairs that are spread throughout the matrix as small agglomerations. High temperatures energise the galvanic activities of these pairs, thus accelerating the oxidation and corrosion process. This is equally true for the wear process, where high frictional temperatures induce similar, leading to faster depletion and failure of the contact zone.

At 280 °C isotherm, lower bainite is formed as fine dispersion across the matrix. High temperatures do not lead to grain boundary galvanic activities. Thus, the matrix is hard to corrode by oxidation or by friction.

This observation is consistent in both tests, where samples treated at 280 °C outperformed those at 400 °C. Quenching in liquid nitrogen provided the best performance in this study.

4. Conclusions

In this work, a new high-strength and ductile cast iron was developed using a combined technique of micro-alloying and heat treatment. The performance of the samples was characterised in terms of hardness, corrosion at high temperatures and frictional wear resistance. Based on the experimental results, the following can be concluded:

- The technique of micro-alloying with boron and subsequent quenching in a liquid bath of Pb-Bi-Sn alloy allowed the engineering of unique inter-matrix structures in the cast iron to the desired constituents.
- Using liquid nitrogen as a cooling medium is a new first-time approach, quenching a cast iron from 400 °C without cracks, and it proved to be an effective method of targeted restructuring of the developed high-strength cast iron.
- The best frictional performance was achieved in samples with a multiphase structure with a mixture of 10–15% lower bainite, martensite and 10% residual austenite.
- The cast irons with a bainite-martensitic matrix structure, however, have a more stable friction coefficient (0.28–0.30) in dry sliding conditions.
- The corrosion resistance of bainite-martensitic samples was increased by 1.5 times with the combination of isothermal holding and cryogenic treatment.
- Treating specimens at 280 °C isotherm with subsequent, direct quenching in nitrogen provided the best performance and opened new opportunities for further investigation aiming at direct industrial applications.

References

1. Menga, N.; Bottiglione, F.; Carbone, G. Dynamically induced friction reduction in micro-structured interfaces. *Sci. Rep.* **2021**, *11*, 8094. [CrossRef] [PubMed]

2. Hasanli, R.; Aliyev, I.; Poladov, N.; Azimova, L.; Tagiyev, T. Isothermal transformations in high-strength cast iron. *Sci. Heraldof Uzhhorod Univ. Ser. Phys.* **2022**, *51*, 48–58. [CrossRef]

3. Akinribide, O.J.; Ogundare, O.D.; Oluwafemi, O.M.; Ebisike, K.; Nageri, A.K.; Akinwamide, S.O.; Gamaoun, F.; Olubambi, P.A. A Review on Heat Treatment of CastIron: Phase Evolution and Mechanical Characterization. *Materials* **2022**, *15*, 7109. [CrossRef] [PubMed]

4. Hegde, A.; Sharma, S.; Hande, R.; Gurumurthy, B.M. Microstructure and mechanical properties of manganese-alloyed austempered ductile iron produced by novel modified austempering process. *Cogent Eng.* **2022**, *9*, 2046301. [CrossRef]

5. Zhao, E.J.; Liu, C.; Northwood, D.O. Accelerated Nano Super Bainite in Ductile Iron. *MRS Adv.* **2018**, *3*, 2789–2794. [CrossRef]

6. Popov, A. *Phase and Structural Transformations in Metal Alloys: A Textbook*; Ural Publishing House, University: Ekaterinburg, Russia, 2018; 316p.

7. Chen, Z.; Jing, L.; Gao, Y.; Huang, Y.; Guo, J.; Yan, X. Impact of Cryogenic Treatment Process on the Performance of 51CrV4 Steel. *Materials* **2023**, *16*, 4399. [CrossRef] [PubMed]

8. Liu, C.; Du, Y.; Wang, X.; Hu, Z.; Li, P.; Wang, K.; Liu, D.; Jiang, B. Mechanical and tribological behavior of dual-phase ductile iron with different martensite amounts. *J. Mater. Res. Technol.* **2023**, *24*, 2978–2987. [CrossRef]

9. Bai, J.; Xu, H.; Chen, X.; Cao, W.; Zhang, X.; Xu, Y. Effect of tempering temperature on the wear behaviour of martensitic ductile iron. *Mater. Sci. Technol.* **2023**, *39*, 744–755. [CrossRef]

10. Li, Q.; Huang, X.; Huang, W. Fatigue property and microstructure deformation behavior of multiphase microstructure in a medium-carbon bainite steel under rolling contact condition. *Int. J. Fatigue* **2019**, *125*, 381–393. [CrossRef]

11. Dong, K.; Lu, C.; Zhou, W.; Northwood, D.O.; Liu, C. Wear behavior of a multiphase ductile iron produced by quenching and partitioning process. *Eng. Fail. Anal.* **2021**, *123*, 105290. [CrossRef]

12. Khidasheli, N.; Gvazava, S.; Batako, A.D.L. Cryogen and heat treatments of boron-lacquered high-strength cast iron. *Mater. Proc.* **2023**. [CrossRef]

13. Wasiak, K.; Węsierska-Hinca, M.; Skołek, E. Effect of a Novel Bainitization Quenching & Partitioning Heat Treatment on Multiphase Microstructure Evolution and Properties of Carburized Cr-Mn-Si Alloyed Steel. *SSRN J.* **2022**, *42*. Available online: https://www.researchgate.net/publication/358688003 (accessed on 2 March 2025). [CrossRef]

14. Wen, F.; Zhao, J.; Zheng, D.; He, K.; Ye, W.; Qu, S.; Shangguan, J. The Role of Bainite in Wear and Friction Behavior of Austempered Ductile Iron. *Materials* **2019**, *12*, 767. [CrossRef] [PubMed]

15. Liu, C.; Yang, C.; Yuan, L.; Northwood, D.O. Role of pre-formed martensite on transformation of austempered ductile iron. *Mater. Sci. Technol.* **2017**, *33*, 1819–1828. [CrossRef]

16. Chen, S.; Hu, J.; Shan, L.; Wang, C.; Zhao, X.; Xu, W. Characteristics of bainitic transformation and its effects on the mechanical properties in quenching and partitioning steels. *Mater. Sci. Eng. A* **2021**, *803*, 140706. [CrossRef]

17. Santofimia, M.J.; Van Bohemen, S.M.; Sietsma, J. Combining bainite and martensite in steel microstructures for light weight applications. *J. South. Afr. Inst. Min. Metall.* **2013**, *113*, 143–148.

18. Popelyukh, A.I.; Tyurin, A.G.; Bardin, A.I. Raising the Properties of Steel 30KhGSA by creating a Mixed Martensitic-Austenitic Structure. *Met. Sci. Heat Treat.* **2022**, *63*, 692–696. [CrossRef]

19. Jha, V.K.; Mozumder, Y.H.; Shama, S.; Behera, R.K.; Pattaniak, A.; Sindhoora, L.P.; Sen, S. Dry sliding war system response of ferritic and tempered martensitic ductile iron. *IOP Conf. Ser. Mater. Sci. Eng.* **2015**, *75*, 012009. [CrossRef]

20. Wei, Z.; Wang, W.; Liu, M.; Tian, J.; Xu, G. Comparison of wear performance of bainitic and martensitic structure with similar fracture toughness and hardness at different wear conditions. *Wear* **2023**, *512–513*, 204512. [CrossRef]

21. Luan, N.H.K.; Koizumi, K.; Mizuno, K.; Yamada, Y.; Okuyama, T.; Nakayama, M. Role of Matrix Structure on Impact-Wear Resistance of As-Quenched 27%Cr Cast Iron. *Mater. Trans.* **2022**, *63*, 740–747. [CrossRef]

22. Krawiec, H.; Lelito, J.; Mróz, M.; Radoń, M. Influence of Heat Treatment Parameters of Austempered Ductile Iron on the Microstructure, Corrosion and Tribological Properties. *Materials* **2023**, *16*, 4107. [CrossRef]

23. Eri, O.; Jovanovi, M.; Šidjanin, L.; Rajnovi, D. Microstructure and mechanicalproperties of cunimo austemperedductile iro. *J. Min. Metall.* **2004**, *40*, 11–19.

24. Medyński, D.; Janus, A. Effect of Cr, Mo and Al on structure and selected mechanical properties of austenitic cast iron. *Arch. Foundry Eng.* **2019**, *19*, 39–44. [CrossRef]

25. Guo, H.; Feng, X.; Zhao, A.; Li, Q.; Ma, J. Influence of Prior Martensite on Bainite Transformation, Microstructures, and Mechanical Properties in Ultra-Fine Bainitic Steel. *Materials* **2019**, *12*, 527. [CrossRef]

26. Guo, H.; Fan, Y.P.; Feng, X.Y.; Li, Q. Ultrafine bainitic steel produced through ausforming-quenching process. *J. Mater. Res. Technol.* **2020**, *9*, 3659–3663. [CrossRef]

27. Kawata, H.; Hayashi, K.; Sugiura, N.; Yoshinaga, N.; Takahashi, M. Effect of Martensite in Initial Structure on Bainite Transformation. *Mater. Sci. Forum* **2010**, *638–642*, 3307–3312. [CrossRef]

28. Qian, L.; Li, Z.; Wang, T.; Li, D.; Zhang, F.; Meng, J. Roles of pre-formed martensite in below-Ms bainite formation, microstructure, strain partitioning and impact absorption energies of low-carbon bainitic steel. *J. Mater. Sci. Technol.* **2022**, *96*, 69–84. [CrossRef]

29. Gulapura, A. Thermodynamic modelling of martensite start temperature in commercial steels. *Mater. Sci. Mater. Sci. Eng.* **2018**, 1–48. Available online: https://kth.diva-portal.org/smash/get/diva2:1176624/FULLTEXT02.pdf (accessed on 2 March 2025).

30. Lu, Y.; Yu, H.; Sisson, R.D. The effect of carbon content on the c/a ratio of as-quenched martensite in Fe-C alloys. *Mater. Sci. Eng. A* **2017**, *700*, 592–597. [CrossRef]

31. Yang, K.; Li, Y.; Hong, Z.; Du, S.; Ma, T.; Liu, S.; Jin, X. The dominating role of austenite stability and martensite transformation mechanism on the toughness and ductile-to-brittle-transition temperature of a quenched and partitioned steel. *Mater. Sci. Eng. A* **2021**, *820*, 141517. [CrossRef]

32. Guerra, L.F.V.; Bedolla-Jacuinde, A.; Mejía, I.; Zuno, J.; Maldonado, C. Effects of boron addition and austempering time on microstructure, hardness and tensile properties of ductile irons. *Mater. Sci. Eng. A* **2015**, *648*, 193–201. [CrossRef]

33. Jain, V.; Sundararajan, G. Influence of the pack thickness of the boronizing mixture on the boriding of steel. *Surf. Coat. Technol.* **2002**, *149*, 21–26. [CrossRef]

34. Maulana, M.I.; Syahid, A.N.; Elvira, B.R.; Erryani, A.; Thaha, Y.N.; Rokhmanto, F.; Mori, M.; Yamanaka, K.; Korda, A.A.; Kartika, I.; et al. Effect of boron microalloying on the microstructure, mechanical, and corrosion properties of as-cast biomedical Co–Cr–W–Ni-based alloys. *J. Mater. Res.* **2024**, *39*, 2272–2285. [CrossRef]

35. Dokumaci, E.; Özkan, I.; Önay, B. Effect of boronizing on the cyclic oxidation of stainless steel. *Surf. Coat. Technol.* **2013**, *232*, 22–25. [CrossRef]

36. Sellamuthu, P.; Samuel, D.; Dinakaran, D.; Premkumar, V.; Li, Z.; Seetharaman, S. Austempered Ductile Iron (ADI): Influence of Austempering Temperature on Microstructure, Mechanical and Wear Properties and Energy Consumption. *Metals* **2018**, *8*, 53. [CrossRef]

37. Batra, U.; Ray, S.; Prabhakar, S.R. The Influence of Nickel and Copper on the Austempering of Ductile Iron. *J. Mater. Eng. Perform.* **2004**, *13*, 64. [CrossRef]

38. Khidasheli, N.; Gordeziani, G.; Gvazava, S.; Tavadze, G.; Tabidze, R.; Batako, A.D.L. *Influence of Structural Parameters on the Wear Resistance of ADI During Dry Sliding Friction. Global Congress on Manufacturing and Management*; Springer: Cham, Switzerland, 2022; pp. 109–116.

39. Carbucicchio, M.; Reverberi, R.; Palobarini, G.; Sambogna, G. On the early stages of oxidation of iron borides. *Hyperfine Interact.* **1989**, *46*, 473–479. [CrossRef]

40. Guitar, M.A.; Scheid, A.; Nayak, U.P.; Nakamura, L.; Ponge, D.; Britz, D.; Mücklich, F. Quantification of the Phase Transformation Kinetics in High Chromium Cast Irons Using Dilatometry and Metallographic Techniques. *Metall Mater Trans A* **2020**, *51*, 3789–3801. [CrossRef]

41. Gazda, A. Determination of the optimal austempering parameters of Ni-Cu (Mo,Mn) ductile iron based on CCT and TTT diagrams. *Prace Inst. Odlew.* **2016**, *56*, 133–145. [CrossRef]